

Dewetting Assisted Patterning of Polystyrene by Soft Lithography to Create Nanotrenches for Nanomaterial Deposition

B. Radha and G. U. Kulkarni*

Chemistry and Physics of Materials Unit and DST Unit on Nanoscience, Jawaharlal Nehru Centre for Advanced Scientific Research, Jakkur P.O., Bangalore 560064, India

ABSTRACT Micromolding in capillaries of polystyrene has been carried out using a poly(dimethylsiloxane) stamp, derived from a compact disk (CD) as master, while heating above the glass transition temperature of polystyrene. The resulting pattern contained a replica of the parallel channels but with an important difference that trenches of width ~ 30 nm were found in between. The nanotrenches in polystyrene could be filled with metals by physical vapor deposition and electroless plating. This method finds potential applications in nanoelectronics and nanofluidics.

KEYWORDS: Polystyrene • micromolding in capillaries • soft lithography • nanotrenches • dewetting • metal nanopatterns.

INTRODUCTION

Patterning surfaces at nanometer scale is crucial and necessary for the fabrication of electronic and biological nano devices. In the manufacture of integrated circuits in industry, the scaling of the current photolithographic techniques to below 100 nm is still a pertinent problem, which requires nanopatterning techniques in place of conventional photolithography (1). Sub-100 nm patterning is generally achieved using focused electron (2) or ion beams (3) in lithography processes, or else by writing with a scanning probe (4). These methods, besides being serial and hence time-consuming, also demand sophistication in instrumentation. This explains the importance attached to relatively inexpensive, simpler, and fast lithography for large area such as stamping, which have emerged since more than a decade ago (5, 6). However, the scope of stamping methods for truly nanoscale patterning is rather limited (7). Different variations of soft lithography techniques have emerged addressing this issue (8, 9). The techniques employing capillary forces (10, 11) and mechanical forces (12, 13) have the ability of patterning materials at the nanoscale. Micromolding in capillaries (MIMIC) of polymers is particularly interesting as the polymeric properties such as dewetting could be exploited in pattern generation, particularly in miniaturization of the stamp features. For instance, high resolution features of PMMA, PU and PS have been generated using capillary force lithography (14, 15) by manipulating the initial polymer film thickness. An attempt to miniaturize the feature size by shrinkage of hydrogels was successful leading to an overall reduction in length scale of the pattern by 56% (16). Annealing a film of polystyrene

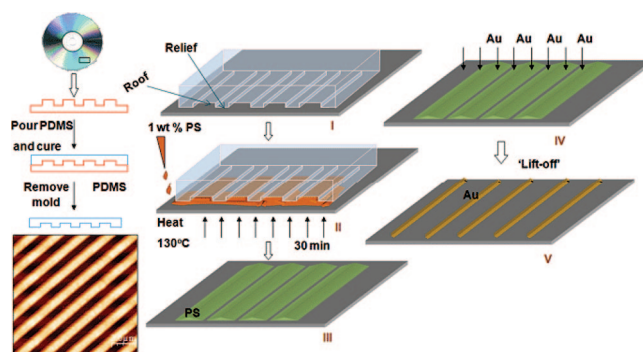


FIGURE 1. Schematic showing the preparation of the PDMS stamp from a CD along with an AFM image of the stamp; molding of polystyrene using the PDMS stamp (steps I–III) and the subsequent metal deposition (steps IV and V) are shown to the right.

above its T_g resulted in controlled dewetting from a PDMS stamp producing features down to ~ 200 nm (17). Herein, we report a simple method based on MIMIC, which exploits the dewetting phenomenon between polymeric surfaces as a means of miniaturizing the patterned feature size in relation to the stamp geometry.

EXPERIMENTAL SECTION

Elastomeric stamps were fabricated in a standard way, by replica molding of polydimethylsiloxane (PDMS) on a commercially available compact disk (Sony CD-R). PDMS was prepared by mixing Sylgard 184 curing agent (Dow Corning) and its elastomer in the ratio of 1:10. This ratio was preferred as it results in a flexible stamp with a Young's modulus of 0.75 MPa and Poisson's ratio of ~ 0.5 (18). The mixture was then degassed under vacuum for 30 min. PDMS was poured onto the master (CD) and then cured in the oven at 70 °C overnight. The stamp peeled off from the master weighed 100 mg and contained line features of 505 nm width separated by 950 nm wide channels. To remove any uncrosslinked low-molecular-weight oligomers, the stamps were cleaned using hexane and sonicated in ethanol for 20 min (19). Si(111) substrates (n-doped, 4–7 Ω cm) and glass slides were cleaned by sonicat-

* To whom correspondence should be addressed. Telephone: 91-80-2208 2814. Fax: 91-80-2208 2766. E-mail: kulkarni@jncasr.ac.in.

Received for review November 8, 2008 and accepted January 16, 2009

DOI: 10.1021/am800172f

© 2009 American Chemical Society

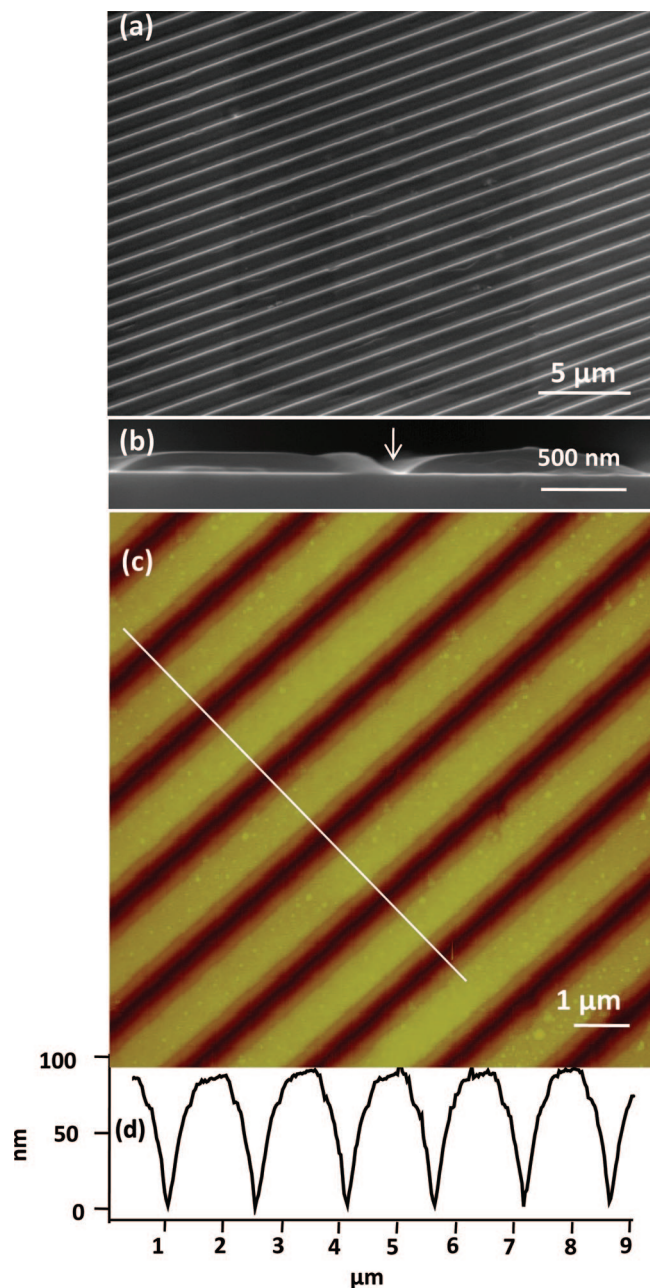


FIGURE 2. (a) FESEM image showing uniform patterning of polystyrene over a large area of Si, (b) cross-section FESEM image showing the groove formation, (c) AFM image showing bright stripes gradually fading into dark grooves, and (d) The AFM z-profile of the pattern.

ing them in acetone and double-distilled water and dried under flowing argon. They were cleaned further by heating at 80 °C in piranha solution (1:2 of H_2O_2 : H_2SO_4) (**Caution:** *this mixture reacts violently with organic matter*) for 10 min. The patterning of polystyrene ($M_w = 260\,000$) consisted of three steps (see Figure 1). PDMS stamp is kept on the Si or glass substrate so that the relief features on the surface of the stamp formed a set of straight and continuous channels (950 nm wide). The stamp along with the substrate was placed on a heating stage. A 60 μL of the polystyrene (PS) solution (1 wt % in toluene) was dropped at one edge of the stamp to fill in the channels spontaneously by capillary action. The setup was then heated to reach 130 °C in ~ 2 min and held at that temperature for 30 min. Following cooling to room temperature, the stamp was removed leaving behind the polymeric patterns on the substrate. Resistive evaporation of Au metal onto the PS patterned

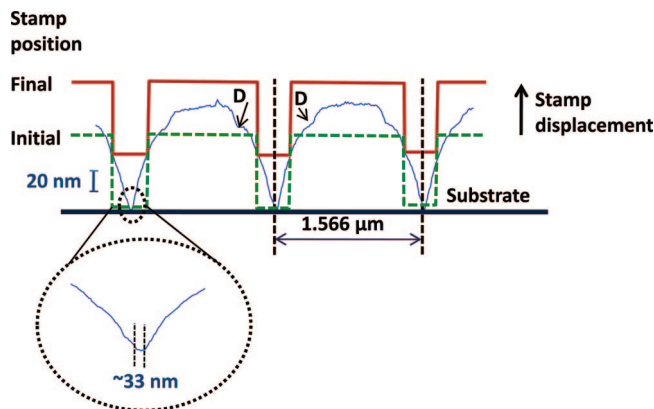


FIGURE 3. AFM z-profile of the PS pattern from Figure 2d (blue) in conformity with stamp geometry (red). The center-to-center distance of the relief features on the stamp matches the feature size of the PS pattern. The PDMS stamp on the substrate before (dotted line) and after (solid line) the creep flow of PS. The gap below the relief features is shown magnified. The regions of high dewetting are shown by arrows marked D.

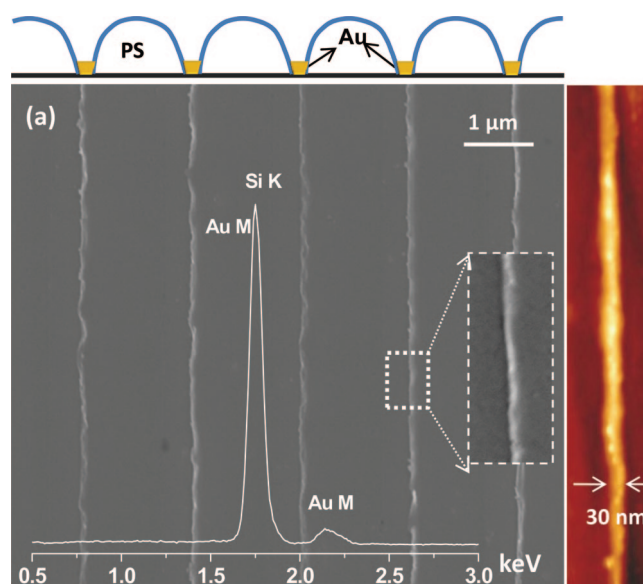


FIGURE 4. Au metal lines formed by physical vapor deposition of the metal onto the polystyrene pattern followed by lift-off of the polymer in toluene. The corresponding EDS spectrum is shown. The associated schematic diagram shows the deposited metal in the groove. The inset shows a higher magnification of a single Au line. AFM image is also shown alongside.

Si substrate was done using a thin film deposition system (HindHi Vac., Bangalore) at a base pressure of 1×10^{-6} torr. The substrate was held directly facing the tungsten basket containing Au fillings, at a distance of ~ 12.5 cm. Lift-off of the polymer was carried out in toluene (1 min). The patterned substrates were examined using a Nova NanoSEM 600 instrument (FEI Co., The Netherlands). Energy-dispersive spectroscopy (EDS) analysis was performed with an EDAX Genesis instrument (Mahwah, NJ) attached to the SEM column. AFM measurements were done using Dimension 3100 SPM with NS-IV controller (Veeco, USA) in the contact mode. Standard Si_3N_4 cantilevers were used for the normal topography imaging.

RESULTS AND DISCUSSIONS

FESEM and AFM micrographs of the polymer pattern on the Si substrate are shown in the Figure 2. In the SEM image in Figure 2a, a set of parallel lines are seen in which the

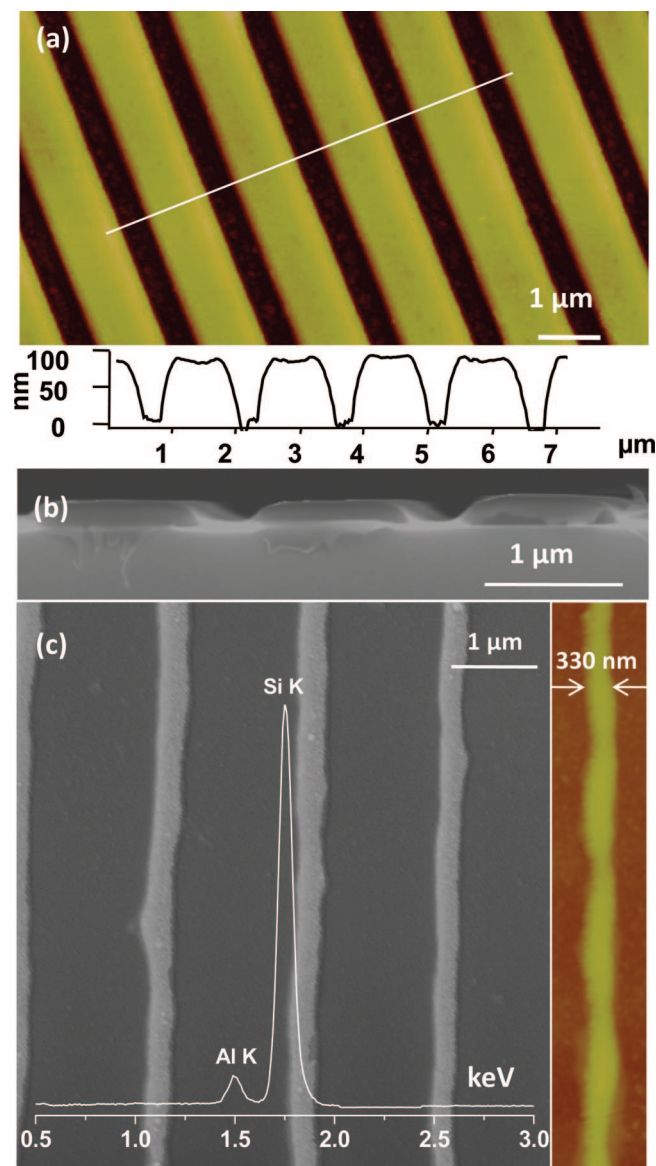


FIGURE 5. (a) AFM micrograph of the PS pattern obtained by the thicker stamp. z-profile is shown below. Trenches of ~ 336 nm width are seen. (b) FESEM cross-section image of the pattern, (c) Al metal lines formed by physical vapor deposition of the metal onto the PS pattern followed by lift-off of the polymer in toluene. The corresponding EDS spectrum is shown. AFM image of a single Al line is shown on the right.

bright regions correspond to the Si signal and the dark to PS, as the polymer comprising of carbon has relatively lower electron scattering cross-section compared to Si. A cross-section SEM image (Figure 2b) showed clearly the presence of narrow grooves in between the polymer stripes. Obviously, the obtained polymer patterns are quite different from the stamp features. Conventional micromolding on the other hand, gives the replica of the stamp features (see Supporting Information, Figure S1) which is evidently not the case here. The topography is more evident from the AFM image shown in Figure 2c. In the image are seen wide bright stripes separated by narrow dark regions. The z-profile (Figure 2d) revealed the cross section of bulged polymer stripes (~ 1.56 μm wide, 90 nm high) separated from each other with narrow V-shaped grooves in between. The groove width as

measured from the z-profile varied from ~ 30 nm at the bottom to ~ 500 nm at the top (20).

It is indeed surprising that the relief features of the stamp instead of blocking the polymer entry seem to allow it to some extent (see Figure 3). In this experiment, the stamp and the substrate were heated to a temperature (~ 130 $^{\circ}\text{C}$) higher than the glass transition temperature of the polymer, T_g (~ 94 $^{\circ}\text{C}$). During the annealing process, the glassy polymer occupying the microchannels formed between the stamp relief features and the substrate dewets the internal PDMS stamp surface due to interfacial forces (21). This effect seems to be maximum at the corners of the roof-relief structures (see arrows marked by D in Figure 3). The dewetting can force the polymer to creep below the stamp relief features (see Figure 3 for details). The creeping being incomplete, V-shaped grooves (trenches) emerge in the polymeric layer. Here, we recall the work of Kim and Lee (17), who heated a film of PS beyond T_g while imprinting with a sharp edged PDMS stamp and obtained nanometric trenches. The work presented here, however, relates to miniaturization of the features and is also different from the capillary force lithography in that it not only employs capillarity but importantly makes use of interfacial dewetting forces to create nanotrenches. Also, it does not call for an additional step of reactive ion etching. The V-groove formation found in this study may not have much to do with possible swelling of the PDMS stamp by the solvent. Toluene is known to swell PDMS (swelling ratio, $S = 1.31$) when the exposure is typically spanning several hours (19). In our experiment, the setup is heated to 130 $^{\circ}\text{C}$ within ~ 2 min of injecting the PS solution and therefore, there is hardly any time for toluene to cause swelling before being evaporated. When the solution was made to evaporate at room temperature after injecting at the stamp-substrate interface (instead of heating to 130 $^{\circ}\text{C}$), we found the replica patterns in conformity with the stamp, typical of conventional micromolding (see the Supporting Information, Figure S1). There was no observable distortion which could be attributed to swelling. Also, we do not expect interference from uncured PDMS in the groove formation, as the uncured polymer species, however, little might be, must have been washed away during the stamp cleaning process (see the Experimental Section).

We anticipated possible opening to the substrate surface at the apex of V-shaped trenches and carried out metal deposition on the patterned PS surface. Physical vapor deposition (PVD) of Au was performed on the PS pattern and following lift-off, narrow line features of width ~ 30 nm and thickness ~ 18 nm, were clearly visible as shown in the FESEM and AFM images of Figure 4, thus establishing the presence of nanogaps. The Au patterns are not strictly linear, but show mild irregularity, perhaps born out of the roughness at the gap boundaries of the PS pattern (see Figure S2 in the Supporting Information).

As the groove formation is a result of the limited creeping of the polymer below the relief features, an increase in the weight of the stamp should reduce creeping and thereby

widen the groove. Indeed, a slightly thicker stamp weighing 150 mg (with similar contact area) produced wider grooves (~ 336 nm) as shown in AFM and cross-section FESEM images a and b in Figure 5, respectively. Al metal was deposited on this PS pattern and the resulting pattern following lift-off contained lines of width ~ 330 nm as shown in FESEM and AFM images in Figure 5c (also see a tilted image in Figure S3 of the Supporting Information). The line thickness is somewhat intermediate to the width of the Au lines shown in Figure 4 and those that result from conventional micromolding. A finer control of the line thickness, however, was not possible under the experimental conditions adopted.

The Au deposition was also brought about by dipping PS patterned Si substrate into a plating solution for 10 min. Here, PS served as a mask allowing Au deposition to take place along the gap lines (see Figure S4 in the Supporting Information). An added novelty of this method is that the PS patterns can be produced on other substrates such as glass (see Figure S5 in the Supporting Information).

CONCLUSIONS

In summary, this study has demonstrated how conventional micromolding in capillaries (MIMIC) can be modified to give rise to nanoscale patterns making use of the dewetting behavior at polymer interfaces. The method produced line features of PS separated by V-shaped grooves. Our method deviates from the conventional MIMIC, in that the polymer being cooled from above its glass transition temperature (94 °C), dewets from the internal PDMS surface and creeps below the relief features. As the creeping does not reach completion, it produces V-shaped grooves with tiny gaps at the apex. The formed PS pattern was employed as a mask in PVD of Au and Al metals on the Si substrate. Following lift-off in toluene, we were able to produce metal line features down to 30 nm. By changing the weight of the stamp, some control on the line width is possible. The PS pattern could also be used as a mask for electroless plating of Au. The method is unique in that it can create miniaturized gaps well below 100 nm. In the trenches, the substrate is exposed and is completely devoid of any residual polymeric layer. The obtained patterns could further be used for making the second generation stamps. The method seems to be general and can possibly work for other polymers as well. The formed trenches can be utilized in filling different nanomaterials. These studies may have importance in nanofluidics as well.

Acknowledgment. The authors thank Professor C. N. R. Rao for his constant encouragement. Support from DST,

India, is gratefully acknowledged. R.B. thanks CSIR, India, for financial assistance.

Supporting Information Available: AFM micrograph showing the PS pattern obtained by conventional MIMIC, deconvoluted AFM image of Figure 2, tilted image of the Al metal lines, SEM micrographs showing the Au nanocrystals deposited in the nanotrenches of PS features by electroless deposition method, PS pattern formed on glass substrate (PDF). This material is available free of charge via the Internet at <http://pubs.acs.org>.

REFERENCES AND NOTES

- (1) Skotnicki, T.; Hutchby, J. A.; King, T. J.; Wong, H. S. P.; Boeuf, F. *IEEE Circuits Devices Mag.* **2005**, *21*, 16–26.
- (2) Bhuvana, T.; Kulkarni, G. U. *ACS Nano* **2008**, *2*, 457–462.
- (3) Arshak, K.; Mihov, M.; Arshak, A.; McDonagh, D.; Sutton, D. *24th International Conference on Microelectronics*, Niš, Serbia, May 16–19, 2004; IEEE: Piscataway, NJ, 2004; Vol. 2, pp 459–462.
- (4) David, S. G.; Hua, Z.; Chad, A. M. *Angew. Chem., Int. Ed.* **2004**, *43*, 30–45.
- (5) Gates, B. D.; Xu, Q.; Love, J. C.; Wolfe, D. B.; Whitesides, G. M. *Ann. Rev. Mater. Res.* **2004**, *34*, 339–372.
- (6) Xia, Y.; Whitesides, G. M. *Angew. Chem., Int. Ed.* **1998**, *37*, 551–575.
- (7) Michel, B.; Bernard, A.; Bietsch, A.; Delamarche, E.; Geissler, M.; Juncker, D.; Kind, H.; Renault, J. P.; Rothuizen, H.; Schmid, H.; Schmidt-Winkel, P.; Stutz, R.; Wolf, H. *IBM J. Res. Dev.* **2001**, *45*, 697–719.
- (8) Geissler, M.; McLellan, J. M.; Xia, Y. *Nano Lett.* **2005**, *5*, 31–36.
- (9) Li, H. W.; Muir, B. V. O.; Fichet, G.; Huck, W. T. S. *Langmuir* **2003**, *19*, 1963–1965.
- (10) Kong, J.; Chapline, M. G.; Dai, H. *Adv. Mater.* **2001**, *13*, 1386–1389.
- (11) Kim, E.; Xia, Y.; Whitesides, G. M. *Nature* **1995**, *376*, 581–584.
- (12) Kim, Y. S.; Suh, K. Y.; Lee, H. H. *App. Phys. Lett.* **2001**, *79*, 2285–2287.
- (13) Chou, S. Y.; Krauss, P. R.; Renstrom, P. J. *J. Vac. Sci. Technol., B* **1996**, *14*, 4129–4133.
- (14) Bruinink, C. M.; Peter, M.; Maury, P. A.; De Boer, M.; Kuipers, L.; Huskens, J.; Reinhoudt, D. N. *Adv. Funct. Mater.* **2006**, *16*, 1555–1565.
- (15) Yu, X.; Wang, Z.; Xing, R.; Luan, S.; Han, Y. *Polymer* **2005**, *46*, 11099–11103.
- (16) Das, A. L.; Mukherjee, R.; Katiyer, V.; Kulkarni, M.; Ghatak, A.; Sharma, A. *Adv. Mater.* **2007**, *19*, 1943–1946.
- (17) Kim, Y. S.; Lee, H. H. *Adv. Mater.* **2003**, *15*, 332–334.
- (18) Armani, D.; Liu, C.; Aluru, N. *IEEE Proc. MEMS* **1999**, 222–227.
- (19) Lee, J. N.; Park, C.; Whitesides, G. M. *Anal. Chem.* **2003**, *75*, 6544–6554.
- (20) The reliability of the observed features was examined by deconvoluting the image with the given tip geometry (see the Supporting Information, Figure S2) using SPIP software (<http://www.imagemet.com/>).
- (21) Sylvain, G.; Pascal, D.; Séverine, S.; Sylvain, D.; Séverine, C.; Günter, R.; Moustafa, H.; Samer, A. A.; Thomas, V.; Elie, R. J. *Polym. Sci., Part B: Polym. Phys.* **2006**, *44*, 3022–3030.

AM800172F